J|A|C|S
ARTICLES
Published on Web 06/17/2006

Accurate Length Control of Supramolecular Oligomerization: Vernier Assemblies

Christopher A. Hunter* and Salvador Tomas*

Contribution from the Centre for Chemical Biology, Krebs Institute for Biomolecular Science, Department of Chemistry, University of Sheffield, Sheffield S3 7HF U.K.

Received March 21, 2006; E-mail: c.hunter@sheffield.ac.uk; s.tomas@shef.ac.uk

Abstract: Linear oligomeric supramolecular assemblies of defined length have been generated using the Vernier principle. Two molecules, containing a different number (n and m) of mutually complementary binding sites, separated by the same distance, interact with each other to form an assembly of length ($n \times m$). The assembly grows in the same way as simple supramolecular polymers, but at a molecular stop signal, when the binding sites come into register, the assembly terminates giving an oligomer of defined length. This strategy has been realized using tin and zinc porphyrin oligomers as the molecular building blocks. In the presence of isonicotinic acid, a zinc porphyrin trimer and a tin porphyrin dimer form a 3:4 triple stranded Vernier assembly six porphyrins long. The triple strand Vernier architecture introduced here adds an additional level of cooperativity, yielding a stability and selectivity that cannot be achieved via a simple Vernier approach. The assembly properties of the system were characterized using fluorescence titrations and size-exclusion chromatography (SEC). Assembly of the Vernier complex is efficient at micromolar concentrations in nonpolar solvents, and under more competitive conditions, a variety of fragmentation assemblies can be detected, allowing determination of the stability constants for this system and detailed speciation profiles to be constructed.

Introduction

An important feature of many biological structures is exquisite control of the size of molecular assemblies on the nano- to mesoscale.[1−5] Supramolecular self-assembly offers the prospect of constructing artificial nanoscale objects with a similar degree of control. To date however, the assembly of well-defined structures has been limited to the construction of closed (poly)-macrocyclic cages, where size is controlled by the requirements of ring closure,[6] or the construction of synthetic membrane pores, where size is controlled by the thickness of the membrane that acts as a template.[7,8] In the area of linear supramolecular polymers, the size of the assembly can be modulated by the concentration of monomers or by adding end-capping units, but the product is always a broad statistical distribution of chain lengths.[9−13] Here, we describe a new approach to the self-assembly of linear oligomeric architectures with well-defined lengths that can be programmed into the molecular structures of the components.

The size of the unit cell of some hybrid crystals is dictated by the formation of Vernier structures, wherein the cell dimensions of the two components come into register to define a supercell.[14] Applied to linear molecular assemblies, the Vernier principle provides a simple way of encoding information about the length of the assembly into the structure of the molecules: two linear components of different length bearing evenly distributed and complementary binding sites will interact with each other until they come into register (Figure 1). This mechanism is a priori very appealing because of its simplicity, but a close inspection reveals some drawbacks that may explain the almost total absence of the application of this principle in the literature.[15] In the simplest formulation, the stability of the Vernier construct is determined by the strength of a single-point binding interaction which constitutes the weakest link in the chain (Figure 2a). Second, two different types of oligomer are required, and these must have mutually complementary but different building sites with identical spacings. Two oligomers composed of the same type of building block with self-complementary binding sites will yield only homodimers.[16] Our solution to the first drawback is the triple strand Vernier approach illustrated in Figure 2b. In this architecture, the weakest link is now a cooperative interaction involving two

(1) Gregorio, C. C.; Weber, A.; Bondad, M.; Pennise, C. R.; Fowler, V. M. *Nature* **1995**, *377*, 83−86.
(2) Berger, B.; Shor, P. W. *J. Struct. Biol.* **1998**, *121*, 285−294.
(3) Marshall, W. F.; Rosenbaum, J. L. *J. Cell Biol.* **2001**, *155*, 405−414.
(4) Seeman, N. C. *Nature* **2003**, *421*, 427−431.
(5) Chworos, A.; Severcan, I.; Koyfman, A. Y.; Weinkam, P.; Oroudjev, E.; Hansma, H. G.; Jaeger, L. *Science* **2004**, *306*, 2068−2072.
(6) Seidel, S. R.; Stang, P. J. *Acc. Chem. Res.* **2002**, *35*, 972−983.
(7) Baumeister, B.; Sakai, N.; Matile, S. *Angew. Chem., Int. Ed.* **2000**, *39*, 1955−1958.
(8) Ghadiri, M. R.; Granja, J. R.; Buehler, L. K. *Nature* **1994**, *369*, 301−304.
(9) Moore, J. S. *Curr. Opin. Colloid Interface Sci.* **1999**, *4*, 108−116.
(10) Brunsveld, L.; Folmer, B. J. B.; Meijer, E. W.; Sijbesma, R. P. *Chem. Rev.* **2001**, *101*, 4071−4097.
(11) Zeng, F. W.; Zimmerman, S. C.; Kolotuchin, S. V.; Reichert, D. E. C.; Ma, Y. G. *Tetrahedron* **2002**, *58*, 825−843.
(12) Lehn, J. M. *Polym. Int.* **2002**, *51*, 825−839.
(13) Michelsen, U.; Hunter, C. A. *Angew. Chem., Int. Edit.* **2000**, *39*, 764−767.
(14) Anokhina, E. V.; Vougo-Zanda, M.; Wang, X. Q.; Jacobson, A. J. *J. Am. Chem. Soc.* **2005**, *127*, 15000−15001.
(15) Kelly, T. R.; Xie, R. L.; Weinreb, C. K.; Bregant, T. *Tetrahedron Lett.* **1998**, *39*, 3675−3678.
(16) For an example of oligomer self-sorting see the following: Taylor, P. N.; Anderson, H. L. *J. Am. Chem. Soc.* **1999**, *121*, 11538−11545.

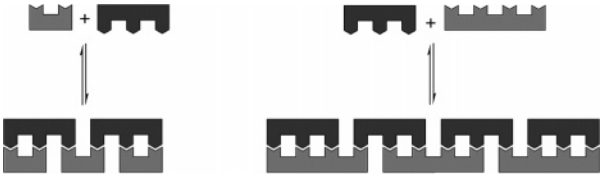

Figure 1. The Vernier mechanism for controlling supramolecular oligomerization. An *n*-mer plus a complementary *m*-mer gives an assembly ($n \times m$) in length.

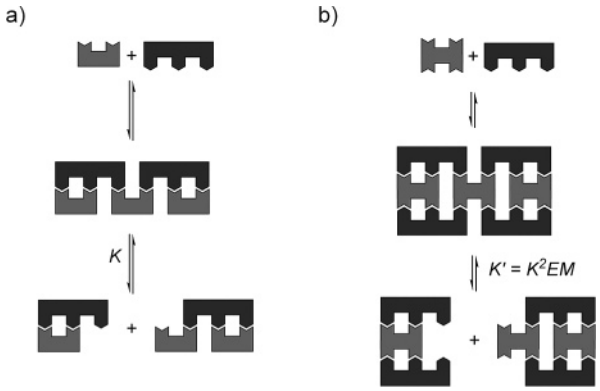

Figure 2. A triple strand Vernier assembly is significantly more stable than a simple double strand Vernier. EM is the effective of molarity of the second intramolecular interaction.

interstrand binding interactions which will lead to a significant increase in stability.[17] We solve the molecular design problem by using linear metalloporphyrin oligomers as the scaffold to correctly position the complementary binding sites on the two different types of component.

Results and Discusion

Porphyrins are widely used in the design of self-assembled systems: it is straightforward to synthesize relatively rigid building blocks with a variety of different types of substituent and to modulate ligand based assembly processes by introducing different metal centers. In this case, monomeric free base porphyrin **H$_2$1** was prepared as described previously[18] and treated with an equimolar amount of terephthaloyl chloride

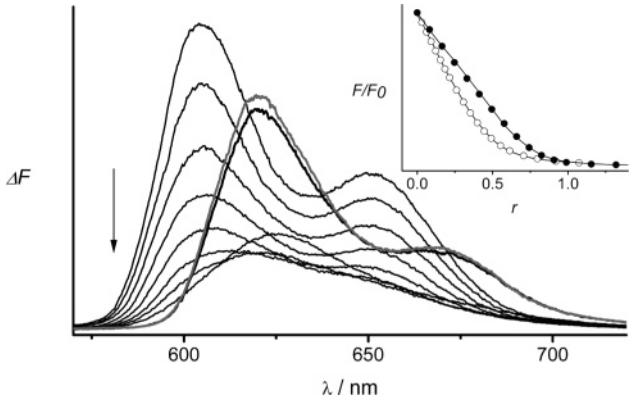

Figure 3. Fluorescence titration of **Zn3** with **Sn2L$_4$** in DCM with 0.05% THF. The spectrum after the addition of excess pyridine to the end point of the titration is shown as the bold line. The gray line is the sum of the individual spectra of **Zn3** and **Sn2L$_4$** at the same concentrations in the same solvent mixture. The inset shows the intensity of fluorescence at 593 nm plotted as a function of *r*, the ratio Sn/Zn porphyrins: empty circles are the **Zn2**-**Sn2L$_4$** titration, filled circles are the **Zn3**-**Sn2L$_4$** titration, and the lines of best fit to the appropriate isotherm are also shown.

yielding a mixture of oligomers of different length (up to hexamer **H$_2$6** was detected by SEC). The dimer and trimer, **H$_2$2** and **H$_2$3**, were isolated by preparative SEC. Reaction of **H$_2$2** with $SnCl_2$ yielded the corresponding tin dimer **Sn2**. The tin−carboxylate interaction is sufficiently strong that the tetraisonicotinate complex **Sn2L$_4$** could be isolated on treatment of **Sn2** with isonicotinic acid. Trimer **Zn3** was synthesized by metalation of **H$_2$3** with $Zn(AcO)_2$ and reference dimer **Zn2** by treating **H$_2$2** in the same way (Scheme 1). Thus, two different oligomers (**Sn2L$_4$** and **Zn3**) with complementary binding sites separated by the same distance were obtained, and these should be ideally suited to the formation of a three stranded Vernier assembly (Figure 2b).

^{1}H NMR spectra of mixtures of **Sn2L$_4$** and **Zn3** were too broad to obtain useful information, and in our hands, the assemblies did not survive the conditions required for ionization in the mass spectrometer. However, the assembly properties of the system could be characterized using a combination of fluorescence spectroscopy and size exclusion chromatography.

Scheme 1. Synthesis of Porphyrin Oligomers

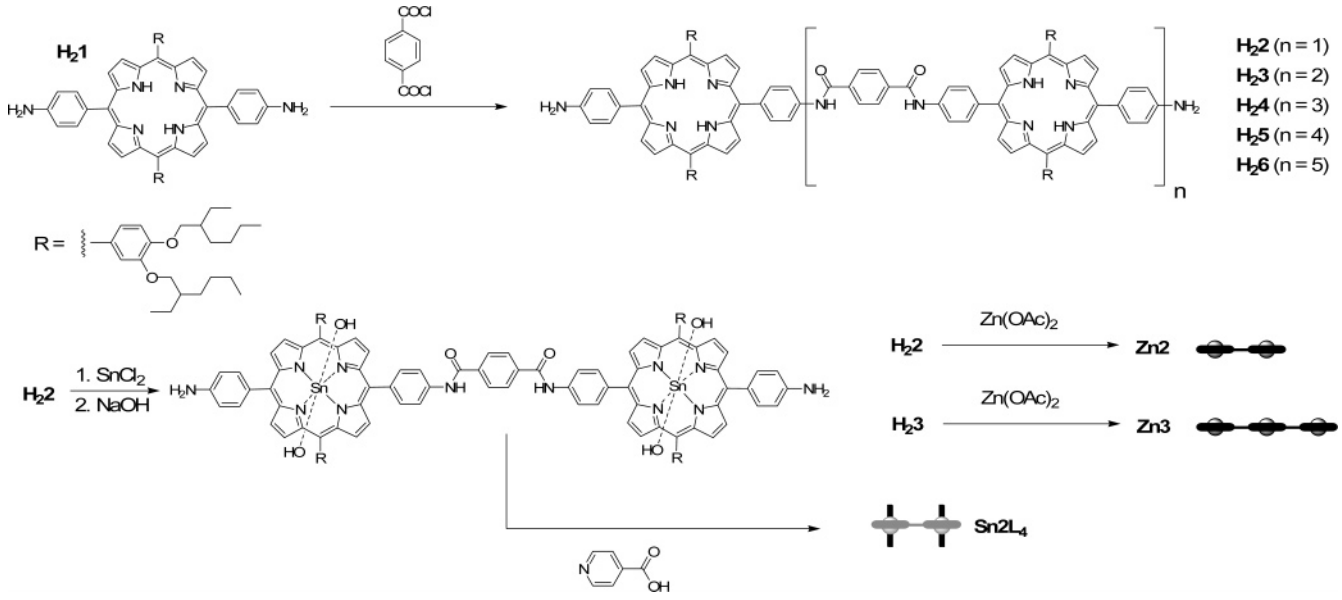

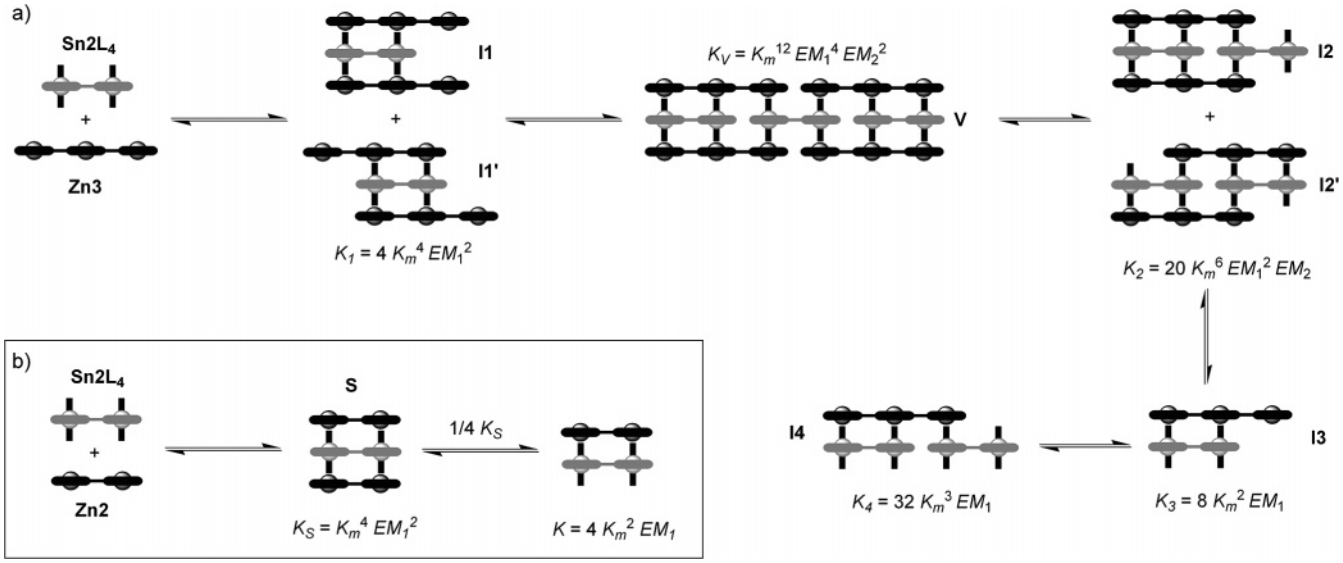

Figure 4. Complexes formed between (a) **Zn3** and **Sn2L$_4$** and (b) **Zn2** and **Sn2L$_4$**. The stability constant of each species is provided in terms of K_m, the microscopic association constant for one zinc−pyridine interaction and the effective molarities EM_1 and EM_2 for the two types of intramolecular interaction. The effective molarities reported here have not been statistically corrected but reflect the overall stability of the assemblies relative to the reference interaction. The statistical factors that are shown reflect the degeneracy of the assembly due to the presence of unoccupied binding sites. K_2 is the overall stability constant for formation of the two complexes of this stoichiometry, so the statistical correction is the sum of a factor of 4 for **I2** and 16 for **I2′**. We assume that there are only two types of intramolecular interaction in the Vernier and that they are independent of the other interactions present, so that just two parameters EM_1 and EM_2 are required to analyze the data.

Table 1. Stability Constants from Fluorescence Titrations[a]

	log $K_m^2EM_1$[b]	log $K_m^2EM_2$[c]	log K_3[d]	log K_1[d]	log K_2[d]	log K_V[d]
DCM/THF 0.05% v/v	7.9 ± 0.2	9.1 ± 0.2	8.8 ± 0.2	16.5 ± 0.4	26.3 ± 0.5	50.0 ± 1.0
SEC eluent[e]	5.5	6.3	6.4	11.6	18.6	34.6

[a] K_m has units of M^{-1},EM of M, K_1 of M^{-2}, K_2 of M^{-3}, K_3 of M^{-1} and K_V of M^{-6}. [b] Determined from titration of **Zn2** with **Sn2L$_4$**. [c] Determined from titration of **Zn3** with **Sn2L$_4$**. [d] Calculated from $K_m^2EM_1$ and $K_m^2EM_2$ and the appropriate statistical corrections (see Figure 4). [e] $CHCl_3$/DMSO/Tetrabuthylammonium, bromide 99.5/0.5/0.5 v/v/w. The errors in these experiments are large because of the weak binding interactions, but the relative stabilites of the species are similar to those found in DCM/THF where the titration data are more reliable.

In dilute solution in dichloromethane, **Zn3** shows a fluorescent emission band at 605 nm upon excitation of either the Soret or Q-band absorptions, and on the addition of pyridine, the emission maximum moved to 620 nm. The corresponding emission wavelength of **Sn2L$_4$** is 620 nm, but selective excitation is not possible because of overlap of the absorption spectra. When increasing amounts of **Sn2L$_4$** were added to a solution of **Zn3**, the intensity of the fluorescent emission at 605 nm decreased until a ratio of 0.75 was reached for [**Sn2L$_4$**]/[**Zn3**]. On the addition of more **Sn2L$_4$**, an increase in fluorescent emission at 620 nm was observed (Figure 3). We interpret the first phase of the titration as the formation of a 3:4 complex in which the emission of the porphyrins is significantly quenched. The second phase of the titration corresponds to the appearance of free **Sn2L$_4$**, which is present in excess. Addition of excess pyridine to the mixture of **Zn3** and **Sn2L$_4$** breaks up the assembly and results in recovery of the fluorescence due to the individual nonassociated species (Figure 3). These experiments show that **Zn3** and **Sn2L$_4$** interact with each other in a reversible fashion to form a stable assembly of the required stoichiometry for the Vernier assembly.

Although the fluorescence titration data can be interpreted naively as the formation of the 3:4 Vernier assembly, there are a series of partially assembled intermediates that may also be present (Figure 4a). There are at least two isomeric forms of each intermediate as illustrated, but unless otherwise specified we will use the terms **I1** and **I2** to refer to the sum of all species with the corresponding stoichiometry. To estimate the stability of these species, we also studied the interactions between the two metalloporphyrin dimers **Zn2** and **Sn2L$_4$**, which can only form the simple triple stranded sandwich assembly shown in Figure 4b. Titration of **Zn2** with **Sn2L$_4$** showed very similar changes in the fluorescence spectra to those observed for **Zn3**, except that assembly was complete after the addition of 0.5 equiv of **Sn2L$_4$** (as expected for formation of a 2:1 sandwich complex). The titration data in dichloromethane with 0.05% v/v tetrahydrofuran fit well to a 2:1 binding model with two equivalent binding events giving a value of 9×10^7 M^{-1} for $K_m^2EM_1$ (see Figure 4, Table 1). This value compares very well with a range of other assemblies we have studied, where two zinc porphyrin−pyridine interactions hold the complex together.[17−19]

Applying the appropriate statistical correction for the presence of unoccupied binding sites in intermediates **I1** and **I3** in Figure 4a, we can use the value of $K_m^2EM_1$ to estimate the stability constants for these species (K_1 and K_3, respectively, see Figure 4a). To estimate the stability of **I2**, we require the association constant for the interaction of **Sn2L$_4$** with **I1**. If we assume that the binding sites on the tin porphyrins in **Sn2L$_4$** are independent, formation of the Vernier assembly from **I1** via **I2**

(17) Hunter, C. A.; Sarson, L. D. *Angew. Chem., Int. Ed. Engl.* **1994**, *33*, 2313−2316.
(18) Haycock, R. A.; Yartsev, A.; Michelsen, U.; Sundstrom, V.; Hunter, C. A. *Angew. Chem., Int. Ed.* **2000**, *39*, 3616−3619.
(19) Camara-Campos, A.; Hunter, C. A.; Tomas, S. *Proc. Natl. Acad. Sci. U.S.A.* **2006**, *103*, 3034−3038.

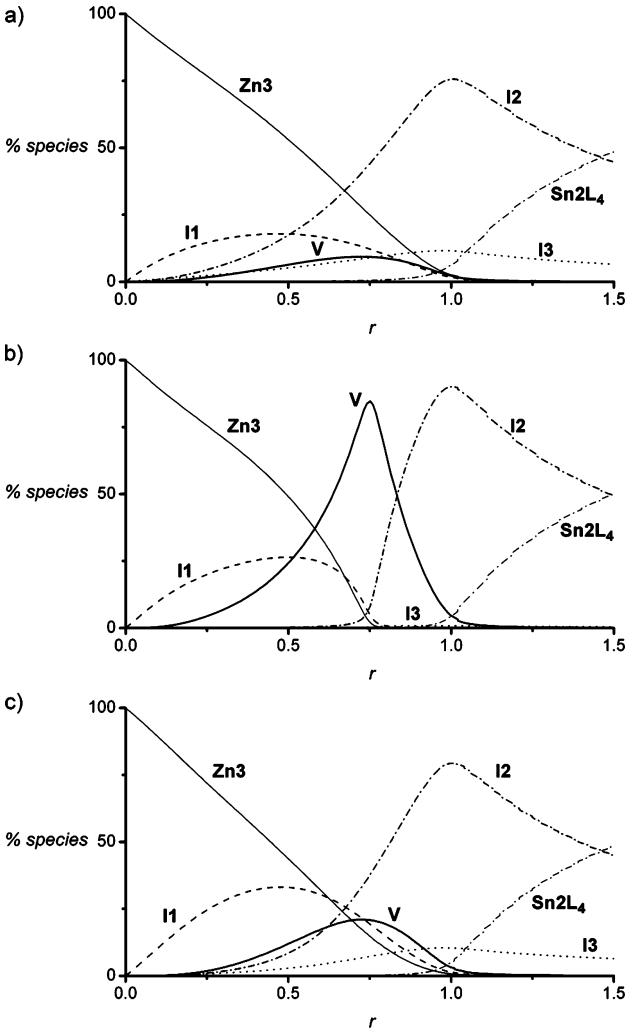

Figure 5. Speciation plots as a function of *r*, the ratio [**Sn2L$_4$**]/[**Zn3**]: (a) [**Zn3**] = 200 nM in DCM with 0.05% THF (fluorescence titration conditions); (b) [**Zn3**] = 50 μM in DCM with 0.05% THF; (c) [**Zn3**] = 250 μM in chloroform with 0.5% v/v DMSO and 0.5% w/v tetrabutylammonium bromide (SEC conditions).

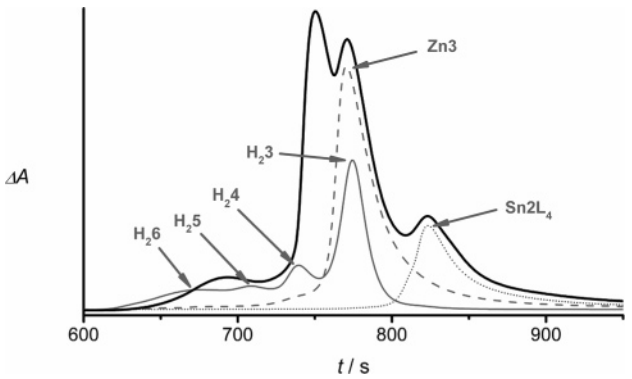

Figure 6. SEC chromatograms of **Sn2L$_4$** (dotted line) and **Zn3** (dashed line), a mixture of **Sn2L$_4$** and **Zn3** (r = 0.75, [**Zn3**] = 150 μM, bold line), and the mixture of covalent oligomers, **H$_2$3**−**H$_2$6** (grey line).

involves two sequential binding events with identical microscopic association constants. In other words, if we use the experimentally determined value of $K_m^2EM_1$ from the triple stranded dimer sandwich, the titration data for formation of the 4:3 assembly can be analyzed using a single variable parameter, the association constant for the interaction of **Sn2L$_4$** with **I1**, $K_m^2EM_2$. The overall stability constants for **I2** and **V**, K_2 and

Table 2. Radius of Gyration (R_g) in nm and Predicted and Experimental SEC Retention Times (r.t.) in Seconds

	Sn2L4	Zn3	I3	I1	I1′	Ladder	I2	I2′	V
R_g[a]	1.52	2.12	2.11	2.29	2.65	2.72	2.75	2.82	3.73−4.67
r.t. calcd[b]	800	776	776	768	754	751	749	747	670−709
r.t. expt	827	773			742				695

[a] Determined from molecular models using the program Hydropro (see ref 20). [b] Determined using the covalently linked oligomer calibration. See SI for details.

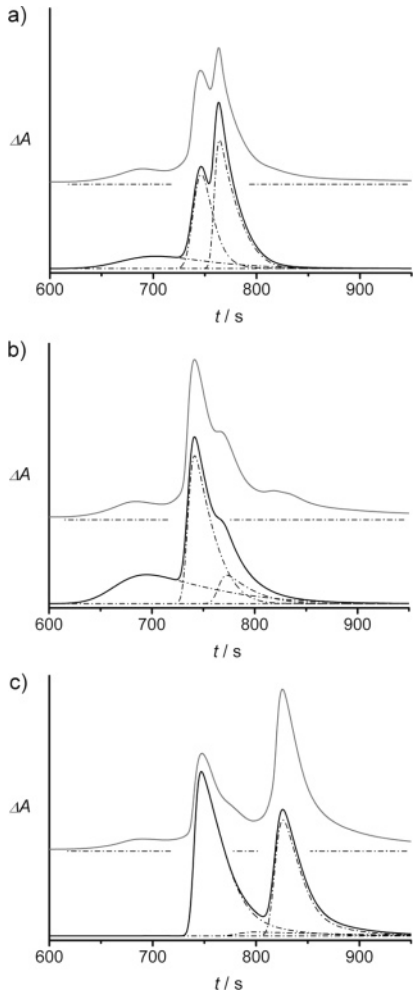

Figure 7. SEC chromatograms at different ratios of [**Sn2L$_4$**]/[**Zn3**]: (a) r = 0.33; (b) r = 0.75; (c) r = 1.75 (total porphyrin concentration = 500 μM). Experimental data are shown in gray and simulated traces are shown in black along with the deconvoluted contributions to each peak.

K_V, respectively, are defined in Figure 4a. The dissociation of these assemblies involves the breaking of two Zn−N interactions, but **I4** would dissociate into **I3** and **Sn2L$_4$** by the removal of a single Zn−N interaction ($K \approx 10^3$ M^{-1}), so **I4** is not present under the experimental conditions (<100 μM). Only zinc porphyrins that are not coordinated to pyridine have a detectable fluorescent emission at 590 nm, so the titration data at this wavelength can be analyzed in terms of three colored species, **Zn3**, **I1** (which we assume has an emission intensity $^2/_3$ of that of **Zn3** in proportion to the number of free zinc porphyrins), and **I3** (which correspondingly has an emission intensity $^1/_3$ of that of **Zn3**). The experimental data in dichloromethane with 0.05% v/v tetrahydrofuran gave an excellent fit to this model (Figure 3 inset), yielding a value of 1×10^9 M^{-1} for the only variable parameter, $K_m^2EM_2$. When the corresponding speciation

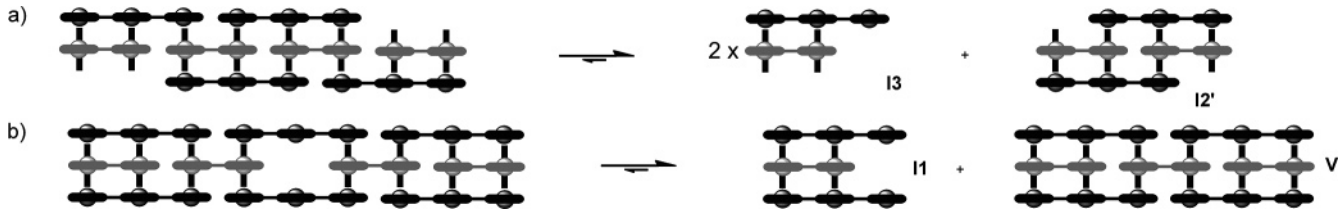

Figure 8. (a) Large assemblies held together by a single Zn−N interaction at the weakest point dissociate into smaller assemblies at the concentrations studied. (b) Large assemblies held together by more than one interaction dissociate into two smaller assemblies that contain the same number of interactions.

profile is analyzed (Figure 5a), it is clear that there are significant proportions of intermediates present at the concentration used for the titration (200 nM). The 4:3 assembly only reaches 15% assembly before destruction by excess **Sn2L$_4$** takes place. However, at a concentration of 50 μM, the 4:3 complex is the major species present at the appropriate stoichiometry (Figure 5b).

Further evidence for the 4:3 assembly was obtained from size exclusion chromatography. Clean well-resolved HPLC−SEC traces of mixtures of **Sn2L$_4$**/**Zn3** could be obtained in chloroform containing 0.5% v/v dimethyl sulfoxide and 0.5% w/v tetrabutylammonium bromide. The stoichiometric ratio required for formation of the Vernier assembly ($r = 0.75$) resulted in a chromatogram with four resolved peaks, indicative of the presence of at least four species in equilibrium (Figure 6). The corresponding chromatogram of the mixture of covalently linked porphyrin oligomers obtained from the first step of the synthesis shown in Scheme 1 provides a convenient calibration of the SEC retention times (Figure 6). Two of the SEC peaks in the **Sn2L$_4$**/**Zn3** mixture can be assigned to the dissociated components **Zn3** and **Sn2L$_4$**, but there are two new species in the chromatogram that have lengths comparable to the covalent tetramer and hexamer. We assign these peaks to the intermediates **I1′**, **I2**, and **I2′**, which are the length of a tetramer, and the Vernier assembly **V**, which is the length of a hexamer. This experiment provides structural evidence for the presence of the Vernier assembly in solution, but the yield is rather low.

The speciation profile under the SEC conditions was estimated by repeating the fluorescence titration experiments described above in chloroform containing 0.5% v/v dimethyl sulfoxide and 0.5% w/v tetrabutylammonium bromide. Although the SEC experiments were carried out at 250 μM concentrations, under these more polar conditions the association constants are significantly reduced (Table 1) accounting for the low population of the Vernier peak in the chromatograms. The speciation profile in Figure 5c suggests that eight different species should be present in detectable amounts under the SEC conditions. The retention times for these species can be estimated crudely based on length: **Sn2L$_4$** is a dimer, **Zn3**, **I1**, and **I3** are trimers, **I1′**, **I2**, and **I2′** are tetramers, and **V** is a hexamer. Alternatively, models can be used to estimate the radius of gyration, R_g (Table 2),[20,21] but in either case, we clearly predict the presence of four distinct peaks in the chromatogram. The 4:3 Vernier stoichiometry is also consistent with a ladder architecture for the assembly, but the radius of gyration for this complex is similar to that of the tetramer, and so any peaks due to this species would be masked by **I1′**, **I2**, and **I2′** in the chromatogram. Thus, while we cannot rule out the presence of a ladder complex, this structure is clearly not consistent with the hexamer peak observed in the SEC. The speciation profiles generated using the association constants determined by the fluorescence titrations and the UV/Vis absorption spectra of **Zn3**, **Sn2L$_4$**, and **V** can be used in conjunction with deconvolution of the experimental SEC trace to predict the appearance of the SEC chromatograms at different ratios of the Vernier components. The results are compared with the corresponding experimental data in Figure 7, and the agreement is very good. In the presence of excess **Zn3**, the major species are **I1′**, **I1**, and free **Zn3**, so we see trimer and tetramer peaks with no dimer. In the presence of excess **Sn2L$_4$**, the major species are **I2**, **I2′**, and free **Sn2L$_4$**, so we see dimer and tetramer peaks with no trimer. At the 4:3 stoichiometry, the extent of Vernier assembly reaches a maximum of 20% under these rather competitive conditions.

Larger assemblies could be formed, if the porphyrin oliogmers slipped out of register (Figure 8), but these are not observed in the SEC chromatograms (Figure 6). In most instances, these larger structures would be held together by a single Zn−N interaction at the weakest link (Figure 8a), and as explained above for **I4**, these interactions would not persist at the concentrations studied. This is not the case for the larger assembly shown in Figure 8b which would appear as a nonamer in the SEC chromatogram in the presence of excess **Zn3**. This species is not observed, because it is more favorable to dissociate into the two smaller assemblies, **I1** and **V**, that contain the same number of interactions.

Concluding Remarks

In summary, we have described the first example of the programmed assembly of a discrete supramolecular oligomer of well-defined length via the Vernier mechanism. The triple-strand approach provides the assembly with enough stability to allow detection of the Vernier complex by SEC at micromolar concentrations in a competitive solvent mixture and allows exclusive formation of the Vernier at the approriate stoichiometry in dichloromethane. Our efforts are currently focused on the development of different building blocks that will provide access to a range of assemblies of different length.

Acknowledgment. We thank the EU (S.T.) and the Lister Institute (C.A.H.) for funding.

Supporting Information Available: Experimental method containing synthetic procedures, molecular modeling simulations, detailed procedures for calibration of the SEC retention times, and simulation of SEC traces in pdf format. This material is available free of charge via the Internet at http://pubs.acs.org.

JA061928F

(20) Garcia de la Torre, J.; Huertas, M. L.; Carrasco, B. *Biophys. J.* **2000**, *78*, 719−730.
(21) Sun, T.; Chance, R. R.; Graessley, W. W.; Lohse, D. J. *Macromolecules* **2004**, *37*, 4304−4312.